AIP Journal of Applied Physics

Effect of growth temperature on the electric properties of In 0.12 Ga 0.88 As/GaAs p-i-n multiple-quantum-well diodes

J. F. Chen, P. Y. Wang, J. S. Wang, and H. Z. Wong

Citation: Journal of Applied Physics **87**, 8074 (2000); doi: 10.1063/1.373500
View online: http://dx.doi.org/10.1063/1.373500
View Table of Contents: http://scitation.aip.org/content/aip/journal/jap/87/11?ver=pdfcov
Published by the AIP Publishing

JOURNAL OF APPLIED PHYSICS VOLUME 87, NUMBER 11 1 JUNE 2000

Effect of growth temperature on the electric properties of $In_{0.12}Ga_{0.88}As/GaAs$ *p-i-n* multiple-quantum-well diodes

J. F. Chen, P. Y. Wang, J. S. Wang, and H. Z. Wong
Department of Electrophysics, National Chiao Tung University, Hsinchu, Taiwan, Republic of China

(Received 10 June 1999; accepted for publication 21 February 2000)

The electric properties of $In_{0.12}Ga_{0.88}As/GaAs$ *p-i-n* multiple-quantum-well (MQW) diodes, with the MQW layer grown at different temperatures by molecular beam epitaxy, have been investigated. Temperature-dependent current–voltage studies reveal a trap-filled limit current at a low temperature and a generation-recombination current via deep levels at high temperature for a 300 °C-grown sample. Frequency-dependent capacitance and deep-level transient spectroscopy reveal one majority trap at 0.73 eV and two minority traps at 0.71 and 0.43 eV. The 0.73 eV trap is also detected in 550 °C-grown samples, suggesting that it is a common defect in relaxed InGaAs/GaAs MQWs and probably originates from the defect states related to the strain relaxation. The 0.71 eV trap is believed to be the dominating deep level that governs the current conduction due to the activation energy observed in the current–voltage characteristics. © *2000 American Institute of Physics.* [S0021-8979(00)00711-8]

I. INTRODUCTION

The low-temperature (LT)-grown GaAs by molecular beam epitaxy (MBE) has a very high resistivity and a short carrier lifetime.[1,2] The LT growth method has recently been extended to the InGaAs material[3–7] and a reduction of the carrier lifetime[3] has been reported. Tsang *et al.*[6] reported that the Ga vacancies V_{Ga} introduced by LT growth can introduce the compositional disordering for InGaAs/GaAs superlattice. However, most of these studies were performed on $In_{0.53}Ga_{0.47}As$, which is lattice matched to InP. The strained InGaAs/GaAs system is another promising material for high-speed and optoelectronic applications. However, there are few reports on the properties of this material system grown at low temperatures. Moreover, this study is also motivated by our previous observation that the trap signals detected in LT-GaAs[8] by deep level transient spectroscopy (DLTS) were weak, probably due to the nature of carrier depletion which makes filling the traps in the LT layer difficult. The heterostructure's quantum confinement may help confine the carriers and enhance the carrier captivity by traps, which in turn increases the visibility of detecting the traps.

In this article, we first present the temperature-dependent current–voltage ($I-V$) characteristics of the 300 °C-grown $In_{0.12}Ga_{0.88}As/GaAs$ multiple-quantum-well (MQW) diode. The $I-V$ data are discussed in terms of the deep levels in the LT layer. Frequency-dependent capacitance and DLTS measurement are performed to establish the properties of the deep levels. Deep levels observed in LT-grown samples are then compared with those from 500 °C-grown samples to pinpoint their origin.

II. SAMPLE DESCRIPTIONS

Figures 1(a)–1(c) illustrate the structures of the three *p-i-n* samples labeled as 91-LT, 90-N, and 89-P, respectively, which were grown by a Varian Gen-II MBE system on n^+-(001) GaAs substrates. The *i* layer of sample 91-LT is a 30 period $In_{0.12}Ga_{0.88}As/GaAs$ MQW grown at 300 °C. This MQW was inevitably annealed for about half an hour at 550 °C due to the growth of the undoped and top *p*-type layers. Samples 90-N and 89-P have structures similar to the 91-LT except that their MQW periods were reduced to 15 and were grown at 550 °C. An additional 0.5-μm-thick undoped GaAs layer is inserted into the structure to isolate the MQW from one of the electrodes. For the 90-N sample, the MQW is designed to be close to the *n*-type GaAs region for increasing the electron confinement in the quantum wells. For the 89-P sample, the MQW is close to the *p*-type region for increasing the hole confinement. Because the smaller mass for electrons, the well width is increased to 250 Å in the 90-N sample in order to have similar degree of confinement.

III. MEASUREMENTS AND RESULTS

A. $I-V$ characteristics

The $I-V$ studies revealed typical rectified curves at 300 K for all three samples. Although the room-temperature $I-V$ under forward bias did not display any interesting difference, the reverse-bias current for the 91-LT sample was about one order of magnitude higher than the other two samples. The forward $I-V$ characteristics of the 90-N and 89-P samples display recombination current at low voltages from 77 to 300 K because of their ideality factors n being close to 2. At large voltages, both samples show the effects of series resistance as seen from the current bending in Fig. 2. At high temperatures, the forward $I-V$ characteristics are similar for all three samples. However, at low temperatures, the 91-LT displays a large turn-on voltage and a sharp current-increasing region as shown in Fig. 2. This sharp current-increasing region cannot be explained by the recombination current through defects. Because, if it were, the recombination lifetime of the 91-LT would be much longer than those of the 89-P and 90-N samples, and this is contradictory to the general observation

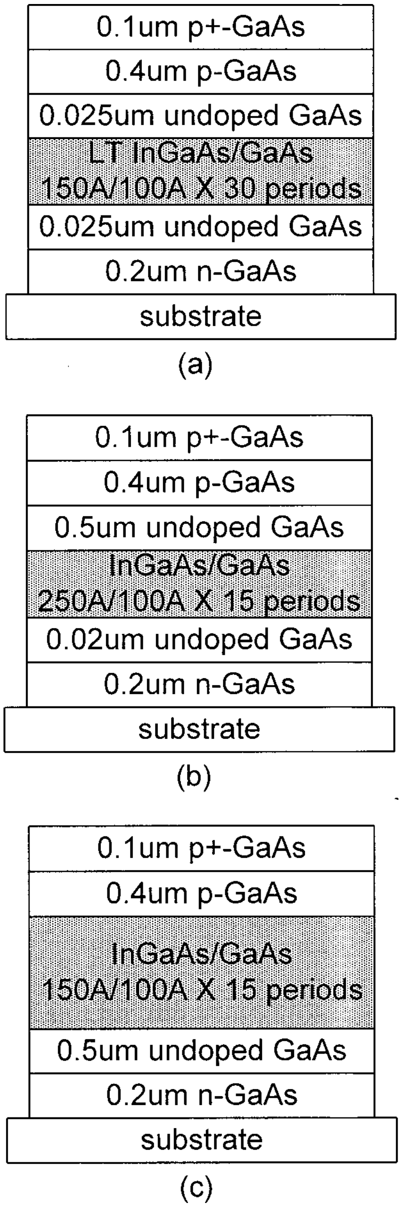

FIG. 1. (a) Structure of the 91-LT sample with $In_{0.12}Ga_{0.88}As$/GaAs MQW grown at a low temperature of 300 °C. (b) Structure of the 90-N sample with MQW close to the *n*-type region and was grown at 550 °C. (c) Structure of the 89-P sample with MQW close to the *p*-type region and was grown at 550 °C.

that the LT-grown sample contains more defects. In addition, the 91-LT displays an ohmic region preceding the sharp current-increasing region. Therefore, the forward current of the 91-LT is believed to exhibit a space-charge-limited current effect. This kind of current conduction is usually observed in materials containing a high density of deep levels.[9,10] The assumption of the existence of deep levels in the MQW region is reasonable because there are at least a 0.3-μ m-thick LT GaAs layer in the 91-LT and a dominating midgap trap[11–14] was always detected in LT GaAs.

Figure 3(a) illustrates the temperature-dependent $I-V$ characteristics of the 91-LT. Because the sample is a $p-n$ junction, the forward current should arise from a double injection of carriers: Holes from p and electrons from n electrodes. We analyze this current conduction in a similar way as reported in Ref. 9. Assuming that this injection process is governed by the deep levels which are acting as recombination centers, the injected electron lifetime τ_n is determined by the concentration p_R of the empty centers: $\tau_n = 1/p_R v_{\mathrm{th}} \sigma_n$ and the injecting hole lifetime by the concentration n_R of the occupied centers: $\tau_p = 1/n_R v_{\mathrm{th}} \sigma_p$ according to Lampert's transport theory.[15] Herein, assume the acceptors in the LT region have a high density, there are few free electrons in the conduction band, and most of the acceptors are in empty states, that is $p_R \gg n_R$. When the carriers are

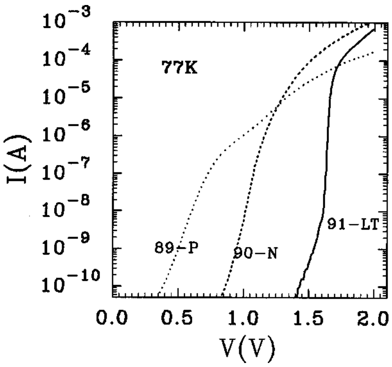

FIG. 2. The forward $I-V$ characteristics at 77 K for 91-LT, 90-N, and 89-P samples. All three samples have 500 μm diameter in area.

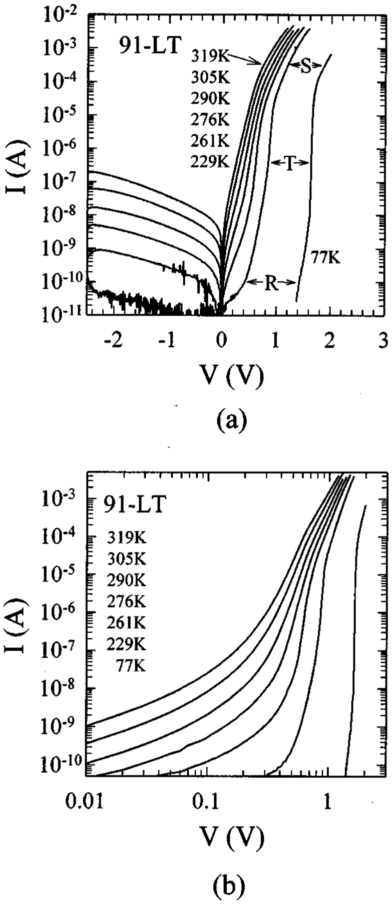

FIG. 3. (a) The $I-V$ characteristics of the 91-LT sample as a function of temperature. (b) The same $I-V$ characteristics of the 91-LT sample but plotted on a linear scale.

injected into the LT region, electrons have a short lifetime and are captured by the empty traps near the *n*-LT edge while holes can travel nearly trap free in the LT region. The current is basically the single hole current that recombines with injected electrons near the *n*-LT edge. This recombination current displays almost ohmic curves [illustrated as ''*R*'' region in Fig. 3(a)], at low voltage under low temperature. The data in Fig. 3(a) are plotted on a linear scale in Fig. 3(b), where the $I-V$ curves are shown to be linear in the *R* region.

The injected holes gradually fill the occupied acceptors when the voltage increases and achieve the trap-filled limit when the acceptors are almost empty. The current will rise strongly with voltage [as illustrated ''*T*'' region in Fig. 3(a)]. This current will continue until it reaches the trap-free space-charge-limited point, beyond which the current increases as $j=\frac{9}{8}\varepsilon\mu_p V_a^2/d^3$. This is illustrated as the ''*S*'' region in Fig. 3(a), where ϵ is the permeability and μ_p is the hole mobility, V_a is the applied bias, and d is the thickness of the LT region. However, it should be noted that the current conduction in this ''*S*'' region could be caused by a series-resistance effect.

Due to thermal excitation, the density of the electrons in the LT region will rise at high temperature and the concentrations of the occupied states will rise also. Therefore, the recombination process is no longer restricted to the *n*-LT edge but extends throughout the whole LT region. Under this condition, the current displays an exponential function in a way similar to the recombination current in a depletion region with midgap defects. The observation of the ideality factor *n* being close to 2 for the $I-V$ curves at high temperature confirms that the current is dominated by this conduction mechanism.

According to the Schockley–Read–Hall recombination theory, the recombination rate can be approximated by $R=n/2\tau_0$, where $n\approx p=n_i\exp(eV_a/2kT)$ assuming a recombination level near the midgap in the LT layer, n_i is the intrinsic carrier concentration, V_a is the applied voltage, and $\tau_0=(\tau_{n0}+\tau_{p0})/2$ is the average recombination lifetime. Assuming $n\approx p$ and the recombination centers are all effective throughout the entire LT region, the recombination current under small bias can be approximated by

$$J_{\text{rec}}\approx\frac{edn_i}{2\tau_0}\exp(eV_a/kT),$$

where $d=0.75\,\mu\text{m}$ is the thickness of the LT region. By fitting the saturation current to the experimental data, an activation energy of about 0.7 eV was obtained. This indicates that the current is indeed attributed by the recombination current in the LT region since it is close to $E_G/2$. By extrapolating the current to zero-voltage axis, we obtained $\tau_0=7.05\times10^{-12}\,\text{s}$ by using $n_i=10^6\,\text{cm}^{-3}$ at 300 K. It should be noted that we might overestimate τ_0 here because the effective recombination thickness must be smaller than the entire LT thickness. A comparison of this value with $\tau_0=9\times10^{-10}\,\text{s}$ from a *p-i-n* GaAs diode previously grown at a normal temperature of 600 °C,[14] proves that this value is almost two orders of magnitude smaller. This short lifetime is consistent with the existence of defect states in the LT region.

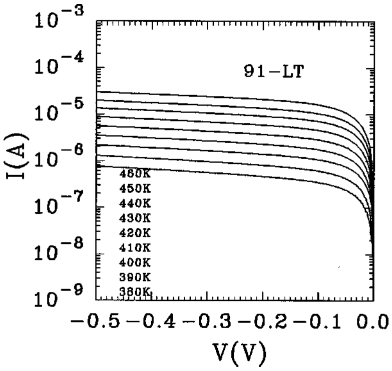

FIG. 4. The reverse $I-V$ characteristics of the 91-LT sample as a function of temperature.

Figure 4 illustrates that the reverse current at small voltage under high temperatures is weakly voltage dependent and displays approximately ohmic behavior. This current conduction can be explained by the generation current via deep levels in the LT region. The slight rise in the current with voltage is attributed to an expansion in the effective width of the LT region. Figure 5 illustrates the Arrhenius plot for the reverse current at several different temperatures. An activation energy of 0.68 eV is obtained for $V=-0.1\,\text{V}$ from the slope of each curve and it decreases slightly to about 0.65 eV for $V=-0.5\,\text{V}$, probably due to field-assisted emission. This activation energy is close to half of the band gap of this material, suggesting that the reverse current is dominated by the generation current from midgap levels.

B. Capacitance–frequency (*C–F*) measurement

Figure 6 illustrates $C-F$ spectra at -1 V for the 91-LT sample. The high-frequency plateau of about 30 pF, from a parallel-plate model, corresponds to the LT thickness. The trap occupation probability is modulated when a small oscillation signal is applied to the diode. If the signal frequency exceeds the trap's emission time, the trap failing to follow this frequency will not change its charge state. Therefore, only the free carriers on both edges of the *n* and *p* regions can be modulated and the measured capacitance corresponds to the width of the total LT region. However, the portion of the traps with energy close to the quasi-Fermi level will alternately capture and emit carriers when the signal frequency

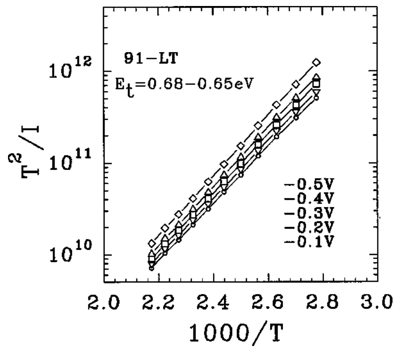

FIG. 5. Arrhenius plot for the reverse current of 91-LT sample at several different temperatures.

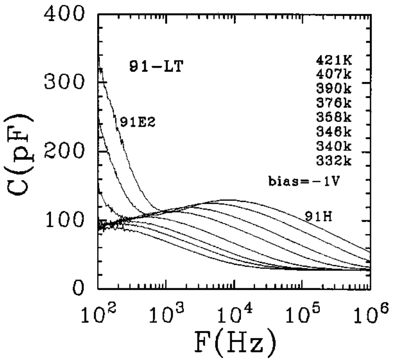

FIG. 6. $C-F$ spectra at a bias of -1 V for 91-LT sample.

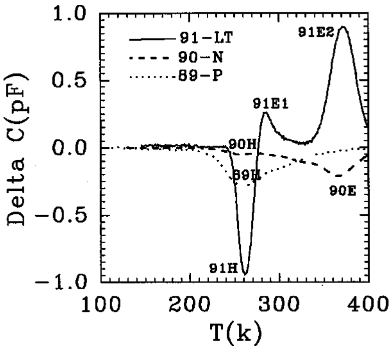

FIG. 7. DLTS data with rate windows 6.4, 6.4, and 5.1 s^{-1} for 91-LT, 89-P, and 90-N samples, respectively. The capacitance transient was measured at -2.5 V bias and the filling pulse was set at 0.1 V with filling pulse time of 3 s.

is sufficiently low. The effective depletion width is reduced, resulting in a rise in the measured capacitance. Figure 6 illustrates that the capacitance increases from a high-frequency 30 pF to a midfrequency 130 pF and further to a low-frequency 350 pF. The rise from the high- to midfrequency value (corresponding to a parallel-plate thickness of 0.17 μm) suggests that a fast trap (labeled as 91H) occupies at least a region of $0.75-0.17=0.58\,\mu$m. The rise from the mid- to low-frequency capacitance (0.06 μm) suggests that a slow trap (labeled as 91E2) occupies at least a region of $0.17-0.06=0.11\,\mu$m. The emission time τ of the trap was determined from the inflexion frequency at which the capacitance step occurs.

The activation energy E_a and capture cross section σ were then achieved by the slope of τT^2 as a function of $1000/T$, yielding the results of 0.71 eV and $1.7\times10^{-11}\,\mathrm{cm}^2$ for the 91H. However, the parameters for the 91E2 cannot be accurately resolved from the $C-F$ spectra because the low-frequency plateau is not clearly defined. Their parameters will be obtained from DLTS measurement.

C. DLTS measurement

Because of the ill-defined nature of defect states in the LT region, we postulate three kinds of charges that could be swept out as based on the three capacitance plateaus in the $C-F$ spectra of Fig. 6: The free carriers on the edges of electrodes as indicated by the high-frequency plateau, carriers emitting from the fast traps (91H) located at about 0.17 μm from one of the LT-electrode interfaces as indicated by the midfrequency capacitance plateau, and the carriers emitting from the slow traps (91E2) located at about 0.11 μm from the LT-electrode interface as indicated by the low-frequency capacitance. Although a high frequency (typically 1 MHz) is normally chosen for DLTS measurement, the capacitance transient related to the latter two cases could be observed in the DLTS measurement with time constants being equal to the reverse of the inflexion frequencies.

Figure 7 presents the DLTS data taken at 30 kHz for all three samples. The 91-LT sample displays very strong signals in contrast to very weak signals previously found in p-LT-n GaAs bulk structures,[8] suggesting an enhancement in the signal visibility by the quantum confinement of carriers. Figure 7 depicts that the 91-LT sample has one majority-carrier trap, 91H, and two minority-carrier traps, 91E1 and 91E2. However, trap 91E1 is overlapped by 91H. The parameters of 91H was resolved without considering any influence by 91E1, but were later slightly modified to provide the best fit for the 91E1. The fitting results are $E_a=0.73\,\mathrm{eV}$, $\sigma=4.6\times10^{-11}\,\mathrm{cm}^2$ for 91H and $E_a=0.43\,\mathrm{eV}$, $\sigma=3.4\times10^{-17}\,\mathrm{cm}^2$ for 91E1, respectively. An $E_a=0.71\,\mathrm{eV}$ with $\sigma=1.5\times10^{-15}\,\mathrm{cm}^2$ was obtained for the minority 91E2 trap. As for 550 °C-grown samples, Fig. 7 illustrates that one majority trap 89H ($E_a=0.74\,\mathrm{eV}$ with $\sigma=1.4\times10^{-11}\,\mathrm{cm}^2$) was detected in sample 89-P and two majority traps at $E_a=0.70\,\mathrm{eV}$ ($\sigma=3.5\times10^{-11}\,\mathrm{cm}^2$) and $E_a=0.77\,\mathrm{eV}$ ($\sigma=8.2\times10^{-15}\,\mathrm{cm}^2$) were detected in sample 90-N. Table I summarizes their results.

It should be noted that the terms of majority and minority traps do not have their conventional meaning because the structures are not conventional n^+-p or p^+-n junctions. We use the term of majority (minority) simply because the transient capacitance increases (decreases) with time. Let us clarify their meanings by a simple model. Considering elec-

TABLE I. Summaries of traps measured by DLTS for $In_{0.12}Ga_{0.88}As/GaAs$ superlattice samples.

	Traps	Kind	T_p (K)	E_a (eV)	Cross section (cm^2)
91-LT	91H	Majority	250	0.73	4.6×10^{-11}
	91E1	Minority	260	0.43	3.4×10^{-17}
	91E2	Minority	370	0.71	1.5×10^{-15}
90-N	90H	Majority	250	0.70	3.5×10^{-11}
	90E	Majority	370	0.77	8.2×10^{-15}
89-P	89H	Majority	250	0.74	1.4×10^{-11}

trons Q_t are emitted out of the traps located in the intrinsic region at a distance of $L_1(L_2)$ from the $p(n)$ electrodes when a reverse voltage is applied. The charge neutrality requires that the changes of ionized charges ΔQ_1 in the p electrode and ΔQ_2 in the n electrode are related by $\Delta Q_1 - Q_t = \Delta Q_2$. Because the applied voltage maintains constant, the total potential drop across the device must be the same before and after Q_t are emitted, that is,

$$\frac{Q_1}{\epsilon} L_1 + \frac{(Q_1+Q_t)}{\epsilon} L_2 = \frac{(\Delta Q_1 + Q_1)}{\epsilon}(L_1+L_2),$$

where $\Delta Q_1 = qp\Delta L_1$ and $\Delta Q_2 = qn\Delta L_2$. Combining the above equations, we obtain

$$\Delta L_1 = \left(\frac{Q_t}{qp}\right)\frac{L_2}{L_1+L_2} \quad \text{and} \quad \Delta L_2 = -\left(\frac{Q_t}{qn}\right)\frac{L_1}{L_1+L_2}.$$

The total variation of the depletion width is given by

$$\sum \Delta L = \Delta L_1 + \Delta L_2 = \frac{Q_t}{q(L_1+L_2)}\left(\frac{L_2}{p} - \frac{L_1}{n}\right).$$

If $\Sigma \Delta L < 0$, the transient capacitance increases with time and the DLTS signal behaves as a majority trap. On the other hand, if $\Sigma \Delta L > 0$, the DLTS signal behaves as a minority trap. Because in our case, the n and p concentrations are about the same order of magnitude, it is possible to observe both the minority and majority traps depending on the relative values of L_1, L_2, which in turn depend on the parameters of the traps.

Detail examination revealed that the traps 91H and 91E2 observed by DLTS were the high- and low-frequency traps observed in $C-F$ spectra, respectively. The trap 91E1 was not detected in the $C-F$ spectra, probably because it is overlapped by 91H and the $C-F$ spectra do not have high resolution for individual traps. The consistency between the $C-F$ and DLTS results indicates that the traps do not result from any capacitance dispersion due to dielectric relaxation[16] or any resistance–capacitance time constant effects.[8,17] Moreover, the parameters of the traps can be more accurately determined because both methods detect traps at very different temperature range.

IV. DISCUSSION

Figure 8 shows the Arrhenius plot for the traps observed by $C-F$ and DLTS measurement. The 91H trap (0.73 eV) is believed to be the same as the 90H and 89H traps. The intensity of this trap is much higher for the 89-P than for the 90-N sample as shown in Fig. 7, suggesting that this trap is a hole trap because the 89-P sample has its MQW region near the p-region and has stronger hole confinement. Since samples 89-P and 90-N were grown at 550 °C, this hole trap is not created solely by the LT growth although its intensity is largest in the LT sample. Therefore, it must be a common defect in a relaxed InGaAs/GaAs MQW. A possible origin of this trap is the strain relaxation due to a lattice mismatch between GaAs and InGaAs. We speculate that our samples are relaxed because their reverse-bias leakage current are more than two orders of magnitude higher than that of the *p-i-n* GaAs bulk samples. A hole trap with an activation energy of 0.67–0.73 eV was reported in relaxed InGaAs/GaAs and was attributed to misfit dislocations.[18] Ashizawa *et al.*[19] observed a trap H2 in their InGaAs/GaAs p^+-n diodes, whose position in the Arrhenius plot (Fig. 8) is close to our 0.73 eV trap. They attributed the H2 to the lattice mismatch between InGaAs and GaAs. Noting that the well width in the sample 90-N is different from the other two samples, indicating that a small variation in the well width does not introduce any significant difference in the parameters of this hole trap.

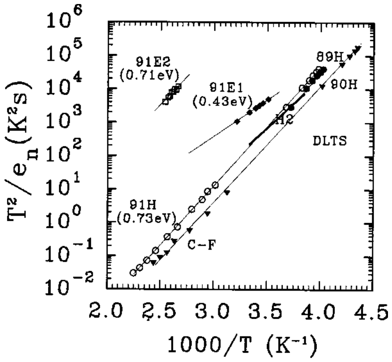

FIG. 8. Arrhenius plot for traps observed in 91-LT, 89-P, and 90-N samples. The hollow squares are 91E2, the solid squares are 91E1 and hollow circles are 91H traps observed in 300 °C-grown 91-LT sample. The solid circles are 89H and solid triangles are 90H traps observed in 550 °C-grown 89-P and 90-N samples, respectively.

The two minority traps at 0.71 and 0.43 eV detected in the 91-LT sample must be related to the LT growth because they were not observed in the 550 °C-grown samples. It is reasonable to deduce that these two traps are electron traps. Adding the activation energies of the 0.71 eV trap and the hole trap at 0.73 eV together renders a value of 1.44 eV that is near the band gap of GaAs at room temperature. This leads us to suspect that they may belong to the same trap. However, the fact that the hole trap but not the 0.71 eV minority trap is discovered in the 550 °C-grown samples excludes the possibility that they belong to the same trap.

The 0.71 eV minority trap is expected to be the important trap that governs the current transport discussed previously. As mentioned before, the $I-V$ characteristics for the 91-LT display a trap-filled-limit current at a low temperature and a generation-recombination current at high temperature. The activation energy of 0.68 eV obtained for the reverse-bias generation current is close to the 0.71 eV. In addition, this midgap trap is speculated to be an important compensation center. We can only refer to those traps reported from LT GaAs because there are few reports on the traps of LT-grown InGaAs/GaAs. A dominating midgap trap was usually detected in LT-grown GaAs, such as those reported by Look *et al.*,[11] by Goo *et al.*[12] from their LT-grown *M-i-n* structures, and by Shiobara *et al.*[13] from their Schottky diodes of LT GaAs. Our previous studies also observed a dominant level at 0.65 eV in LT-GaAs structures.[14] There are two levels in Look's model: the most important compensation center at 0.7 eV and the other at around 0.5 eV to make the annealed LT GaAs highly resistive. Although our observations of 0.71 and 0.43 eV traps support their model, we cannot conclude that our 0.43 eV level is their 0.5 eV level.

V. CONCLUSIONS

Three traps with significant intensity, one majority trap at 0.73 eV and two minority traps at 0.71 and 0.43 eV, have been observed in a LT-grown $In_{0.12}Ga_{0.88}As/GaAs$ MQW sample. The 0.73 eV trap, which is also detected in 550 °C-grown samples, is believed to be a common hole trap in relaxed $In_{0.12}Ga_{0.88}As/GaAs$ MQWs. Among the two traps only observed in LT-grown samples, the 0.71 eV trap is expected to be the most important compensation center and the dominant deep level that governs the current–voltage characteristics.

ACKNOWLEDGMENTS

The authors are grateful to Dr. N. C. Chen for many useful discussions and would like to thank the National Science Council of the Republic of China for financially supporting this research under Contract No. NSC-87-2112-M-009-022.

[1] D. C. Look, D. C. Walters, M. O. Manasreh, J. R. Sizelove, and C. E. Stutz, Phys. Rev. B **42**, 3578 (1990).
[2] A. C. Warren, J. M. Woodall, J. L. Freeouf, D. Grischkowsky, and D. T. Mclnturff, Appl. Phys. Lett. **57**, 1331 (1990).
[3] J. F. Whitaker, Mater. Sci. Eng., B **22**, 61 (1993).
[4] R. Takahashi, Y. Kawamura, T. Kagawa, and H. Iwamura, Appl. Phys. Lett. **65**, 1790 (1994).
[5] P. W. Juodawlkis, D. T. McInturff, and S. E. Ralph, Appl. Phys. Lett. **69**, 4062 (1996).
[6] J. S. Tsang, C. P. Lee, S. H. Lee, K. L. Tsai, and J. C. Fan, J. Appl. Phys. **79**, 664 (1996).
[7] P. K. Bhattacharya, S. Dhar, P. Berger, and F. Y. Juang, Appl. Phys. Lett. **49**, 470 (1986).
[8] J. F. Chen, P. Y. Wang, and N. C. Chen, Jpn. J. Appl. Phys., Part 2 **37**, L1238 (1998).
[9] J. Cheng, S. R. Forrest, B. Tell, D. Wilt, B. Schwartz, and P. Wright, J. Appl. Phys. **58**, 1787 (1985).
[10] J. F. Chen, N. C. Chen, S. Y. Chiu, P. Y. Wang, W. I. Lee, and A. Chin, J. Appl. Phys. **79**, 8488 (1996).
[11] D. C. Look, Z.-Q. Fang, H. Yamamto, J. R. Sizelove, M. G. Mier, and C. E. Stutz, J. Appl. Phys. **76**, 1029 (1994).
[12] C. H. Goo, W. S. Lau, T. C. Chong, and L. S. Tan, Appl. Phys. Lett. **69**, 2543 (1996).
[13] S. Shiobara, T. Hashizume, and Hasegawa, Jpn. J. Appl. Phys., Part 2 **35**, L1159 (1996).
[14] N. C. Chen, P. Y. Wang, and J. F. Chen, J. Appl. Phys. **83**, 1403 (1998).
[15] M. A. Lampert and P. Mark, *Current Injection in Solids* (Academic, New York, 1970).
[16] R. K. Ahrenkiel, P. Sheldon, D. Dunlavy, L. Roybal, and R. E. Hayes, Appl. Phys. Lett. **43**, 675 (1983).
[17] D. V. Lang, M. B. Panish, F. Capasso, J. Allam, R. A. Hamm, A. M. Sergent, and W. T. Tsang, Appl. Phys. Lett. **50**, 736 (1987).
[18] A. Y. Du, M. F. Li, T. C. Chong, K. L. Teo, W. S. Lau, and Z. Zhang, Appl. Phys. Lett. **69**, 2849 (1996).
[19] Y. Ashizawa, S. Akbar, W. J. Schaff, and L. F. Eastman, J. Appl. Phys. **64**, 4065 (1988).